Pre-reactive Complexes in Mixtures of Water Vapour with Halogens: Characterisation of $H_2O\cdots ClF$ and $H_2O\cdots F_2$ by a Combination of Rotational Spectroscopy and Ab initio Calculations

Stephen A. Cooke,[a] Gina Cotti,[a] Christopher M. Evans,[a] John H. Holloway,[b] Zbigniew Kisiel,[c] Anthony C. Legon,*[a] and Jennifer M. A. Thumwood[a]

Abstract: Complexes $H_2O\cdots ClF$ and $H_2O\cdots F_2$ were detected by means of their ground-state rotational spectra in mixtures of water vapour with chlorine monofluoride and difluorine, respectively. A fast-mixing nozzle was used in conjunction with a pulsed-jet, Fourier-transform microwave spectrometer to preclude the vigorous chemical reaction that these dihalogen species undergo with water. The ground-state spectra of seven isotopomers ($H_2{}^{16}O\cdots{}^{35}ClF$, $H_2{}^{16}O\cdots{}^{37}ClF$, $H_2{}^{18}O\cdots{}^{35}ClF$, $D_2{}^{16}O\cdots{}^{35}ClF$, $D_2{}^{16}O\cdots{}^{37}ClF$, $HDO\cdots{}^{35}ClF$ and $HDO\cdots{}^{37}ClF$) of the ClF complex and five isotopomers ($H_2O\cdots F_2$, $H_2{}^{18}O\cdots F_2$, $D_2O\cdots F_2$, $D_2{}^{18}O\cdots F_2$ and $HDO\cdots F_2$) of the F_2 complex were analysed to yield rotational constants, quartic centrifugal distortion constants and nuclear hyperfine coupling constants. These spectroscopic constants were interpreted with the aid of simple models of the complexes to give effective geometries and intermolecular stretching force constants. Isotopic substitution showed that in each complex the H_2O molecule acts as the electron donor and either ClF or F_2 acts as the electron acceptor, with nuclei in the order $H_2O\cdots ClF$ or $H_2O\cdots F_2$. For $H_2O\cdots ClF$, the angle ϕ between the bisector of the HOH angle and the $O\cdots Cl$ internuclear line has the value 58.9(16)°, while the distance $r(O\cdots Cl)=2.6081(23)$ Å. The corresponding quantities for $H_2O\cdots F_2$ are $\phi=48.5(21)°$ and $r(O\cdots F_i)=2.7480(27)$ Å, where F_i indicates the inner F atom. The potential energy $V(\phi)$ as a function of the angle ϕ was obtained from ab initio calculations at the aug-cc-pVDZ/MP2 level of theory for each complex by carrying out geometry optimisations at fixed values of ϕ in the range $\pm 80°$. The global minimum corresponded to a complex of C_s symmetry with a pyramidal configuration at O in each. The function $V(\phi)$ was of the double-minimum type in each case with equilibrium values $\phi_e=\pm 55.8°$ and $\pm 40.5°$ for $H_2O\cdots ClF$ and $H_2O\cdots F_2$, respectively. The barrier at the planar C_{2v} conformation was $V_0=174\,cm^{-1}$ for $H_2O\cdots ClF$ and $7\,cm^{-1}$ for $H_2O\cdots F_2$. For the latter complex, the zero-point energy level lies above the top of the barrier.

Keywords: fluorine · halogen bonds · intermediates · rotational spectroscopy · water chemistry

Introduction

We report here a detailed characterisation of the weakly bound complexes $H_2O\cdots F_2$ and $H_2O\cdots ClF$, as achieved by a combination of rotational spectroscopy and ab initio calculations. Spectra were observed by means of a pulsed-nozzle, Fourier-transform microwave spectrometer[1, 2] equipped with a fast-mixing nozzle.[3] The latter device avoids premature mixing of H_2O and the dihalogen molecule $XY=F_2$ or ClF, ensures that the two components interact with each other in the absence of surfaces (thereby excluding the possibility of heterogeneous reaction), and ensures that the complexes of $H_2O\cdots XY$ achieve collisionless expansion rapidly enough to preclude any homogenous reaction, either bimolecular or unimolecular.

There are two reasons for our interest in $H_2O\cdots F_2$ and $H_2O\cdots ClF$. The first is because of the vigorous and complicated reactions that the simplest homo- and heteronuclear dihalogen molecules F_2 and ClF each undergoes in contact with water. In the case of F_2, it was demonstrated that H_2O_2, O_2, HF and F_2O are among the products,[4, 5] while for ClF,

[a] Prof. Dr. A. C. Legon, Dr. S. A. Cooke, Dr. G. Cotti, Dr. C. M. Evans, J. M. A. Thumwood
School of Chemistry, University of Exeter, Stocker Road
Exeter, EX4 4QD (UK)
Fax: (+44) 1392-263434
E-mail: A.C.Legon@exeter.ac.uk

[b] Prof. Dr. J. H. Holloway
Department of Chemistry, University of Leicester
University Road, Leicester, LE1 7RH (UK)

[c] Dr. Z. Kisiel
Institute of Physics, Polish Academy of Sciences
Al. Lotników 32/46, 02-668, Warszawa (Poland)

  0947-6539/01/0711-2295 $ 17.50+.50/0

depending on the conditions, either HF, Cl_2 and O_2 or HF, ClO_2, Cl_2 and O_2 or HF and Cl_2O are formed.[6] Given the evident complexity of the reactions, which have been summarized elsewhere,[7, 8] and their vigorous nature, it is a significant challenge to chemists to isolate and characterise molecular complexes $H_2O\cdots F_2$ or $H_2O\cdots ClF$ in water/halogen mixtures before reaction can occur. Therefore, preliminary reports[7, 8] of the rotational spectra of these species emphasised their experimental identification and concentrated on establishing the order of the nuclei. In each case, H_2O acts as the Lewis base (electron donor), while F_2 or ClF acts as the Lewis acid (electron acceptor). Such species have been referred to as pre-reactive because the possibility of their existence is terminated by the chemical reactions alluded to.

The second reason for interest in $H_2O\cdots F_2$ and $H_2O\cdots ClF$ lies in their role as simple members of the series $B\cdots F_2$ and $B\cdots ClF$, respectively, where B is one of several Lewis bases. Recently, the series $B\cdots F_2$, $B\cdots ClF$, $B\cdots Cl_2$, $B\cdots BrCl$, $B\cdots Br_2$ and $B\cdots ICl$ have been investigated systematically[9, 10] by rotational spectroscopy to obtain various properties of the complexes and examine how they change as B is varied. As a result, remarkable parallelisms have been identified between the properties of $B\cdots XY$ (where XY is a homo- or heteronuclear dihalogen) and those of the corresponding hydrogen-bonded complexes $B\cdots HX$. In particular, it was shown that for a given Lewis base B the angular geometries of $B\cdots XY$ and $B\cdots HX$ are isomorphous. These parallelisms led one of us to postulate[9, 11] the existence of a halogen bond, $B\cdots{}^{\delta+}X{-}Y^{\delta-}$ or $B\cdots{}^{\delta+}X\frac{\delta-}{\delta-}X^{\delta+}$, that is the analogue of the more familiar hydrogen bond $B\cdots{}^{\delta+}H{-}X^{\delta-}$. Indeed, some rules for predicting angular geometries, originally enunciated for hydrogen-bonded complexes,[12, 13] were extended to include halogen-bonded complexes. One part of these rules requires that in the equilibrium conformation of the complex the ${}^{\delta+}H{-}X^{\delta-}$ or ${}^{\delta+}X{-}Y^{\delta-}$ molecule lies, electrophilic end first, along the axis of a nonbonding electron pair carried by the electron donor atom Z of B. Hence, $H_2O\cdots ClF$ and $H_2O\cdots F_2$ are predicted to possess equilibrium geometries of C_s symmetry in which the ClF or F_2 molecules make an angle of $\phi\approx 50^\circ$ with the C_2 axis of H_2O. We shall use a combination of ab initio calculations with our experimental observations to establish the angular geometries of $H_2O\cdots F_2$ and $H_2O\cdots ClF$. We shall show that the potential energy function $V(\phi)$ is a double-minimum function of the angle ϕ in both cases. Moreover, we shall see that the minima are located at about $\pm 50^\circ$, as required by the rules, even though in the case of $H_2O\cdots F_2$ the potential energy barrier to the planar, C_{2v} conformation is very small. The parallelism in the angular geometries of $B\cdots XY$ and $B\cdots HX$ is shown thereby to extend to $B=H_2O$ and is reflected in similarities in the function $V(\phi)$ for $H_2O\cdots ClF$ and $H_2O\cdots HCl$.

Results

Spectral analyses: The observed ground-state rotational spectra of both $H_2O\cdots F_2$ and $H_2O\cdots ClF$ were of the type expected for a nearly prolate, asymmetric rotor with a large value of the rotational constant A_0. In each case, only R branch transitions $(J+1)_{K_{-1}K_1}\leftarrow J_{K_{-1}K_1'}$ allowed by the *a* component of the electric dipole moment were observed and, of these, only those involving $K_{-1}=0$ and 1 could be detected. The absence of transitions having $K_{-1}\geq 2$ is consistent with a large value of A_0, since levels with $K_{-1}\neq 0$ are higher in energy than the $K_{-1}=0$ state for a given J by $\approx h(A-B)\ K_{-1}^2$ for a nearly prolate rotor. The geometries determined for $H_2O\cdots F_2$ and $H_2O\cdots ClF$ predict A_0 values of about 200–300 GHz and, therefore, $K_{-1}=2$ levels at a wavenumber of about 30–40 cm^{-1}. Such states are unlikely to be populated at the end of the supersonic expansion process for reasons discussed in the next section.

Each rotational transition of the various isotopomers of $H_2O\cdots ClF$ exhibited a hyperfine structure spread over a few tens of MHz that was attributed to nuclear quadrupole coupling of the Cl nuclear spin vector $\boldsymbol{I}_{Cl}$ to the rotational angular momentum vector $\boldsymbol{J}$. Observed frequencies of the hyperfine components in the $J=2\leftarrow 1$ and $3\leftarrow 2$ sets of transitions for the isotopomers $H_2O\cdots{}^{35}ClF$, $H_2O\cdots{}^{37}ClF$ and $H_2{}^{18}O\cdots{}^{35}ClF$ are shown in Table 1, while those for the deuterated isotopomers $D_2O\cdots{}^{35}ClF$, $D_2O\cdots{}^{37}ClF$, $HDO\cdots{}^{35}ClF$ and $HDO\cdots{}^{37}ClF$ are given in Table 2. The small amount of $H_2{}^{18}O$ sample available, coupled with the need to flow this component continuously through the fast-mixing nozzle, meant that only the $J=2\leftarrow 1$ transitions could be measured for $H_2{}^{18}O\cdots{}^{35}ClF$. No effects of D-nuclear quadrupole coupling could be satisfactorily resolved for the deuterated isotopomers and for those based on $HDO\cdots ClF$ transitions involving $K_{-1}=1$ were too weak to observe under the prevailing expansion conditions. Reasons for the weakness of $K_{-1}=1$ transitions of HDO species will be discussed in the next section.

The observed hyperfine frequencies of the various isotopomers of $H_2O\cdots ClF$ were fitted in an iterative least-squares analysis in which the matrix of the Hamiltonian given in Equation (1) was constructed in the coupled symmetric rotor basis $\boldsymbol{J}+\boldsymbol{I}=\boldsymbol{F}$ and the separate F blocks were diagonalized.

$$H=H_R-\tfrac{1}{6}\mathbf{Q}(Cl):\nabla\mathbf{E}(Cl)+\boldsymbol{I}\mathbf{M}(Cl)\boldsymbol{J} \qquad (1)$$

In Equation (1), H_R is the Hamiltonian operator associated with the semi-rigid asymmetric rotor, for which the Watson A-reduction in the I^r representation[14] was chosen. Only the rotational constants B_0 and C_0 and the quartic centrifugal distortion constants Δ_J and Δ_{JK} were determinable, because of the proximity of $H_2O\cdots ClF$ to the prolate symmetric-top limit and the limited range of transitions available. Consequently, Δ_K, δ_K and δ_J were preset to zero, while A_0 was fixed at the value predicted by the final geometry of $H_2O\cdots ClF$, as determined in the next Section. The second term in Equation (1) describes the Cl nuclear quadrupole coupling in the usual way, where $\mathbf{Q}(Cl)$ is the Cl nuclear electric quadrupole moment tensor and $\nabla\mathbf{E}(Cl)$ is the electric field gradient tensor at the Cl nucleus. The final term of Equation (1) takes account of the energy of the magnetic interaction of the Cl nuclear spin angular momentum $\boldsymbol{I}_{Cl}$ with $\boldsymbol{J}$, where $\mathbf{M}(Cl)$ is the chlorine spin-rotation coupling tensor.

  0947-6539/01/0711-2296 $ 17.50+.50/0 *Chem. Eur. J.* **2001**, *7*, No. 11

Table 1. Observed and calculated rotational transition frequencies of $H_2O\cdots{}^{35}ClF$, $H_2O\cdots{}^{37}ClF$ and $H_2{}^{18}O\cdots{}^{35}ClF$.

$J'_{K_{-1}K_1} \leftarrow J''_{K_{-1}K_1}$	F'	←	F''	$H_2O\cdots{}^{35}ClF$		$H_2O\cdots{}^{37}ClF$		$H_2{}^{18}O\cdots{}^{35}ClF$	
				ν_{obs} [MHz]	$\Delta\nu$[a] [kHz]	ν_{obs} [MHz]	$\Delta\nu$[a] [kHz]	ν_{obs} [MHz]	$\Delta\nu$[a] [kHz]
$2_{02} \leftarrow 1_{01}$	7/2		5/2	11647.4423	1.4	11642.0526	−5.1	10967.9361	6.5
	5/2		3/2	11647.4172	−6.0	11642.0526	7.3	10967.9064	−5.5
	3/2		1/2	11607.5959	−4.1	–	–	–	–
	5/2		5/2	11610.6951	0.5	11613.0922	3.6	–	–
	3/2		3/2	11673.7521	−1.8	11662.7797	−2.7	10994.2467	−3.3
	1/2		1/2	11644.2614	−1.5	11639.5516	−1.0	10964.7564	2.3
$2_{11} \leftarrow 1_{10}$	7/2		5/2	11672.5204	4.9	11665.8987	2.4	10990.8736	0.9
	5/2		3/2	11635.8294	−2.0	11636.9571	−8.3	10954.2028	7.1
	3/2		1/2	11682.2052	−1.8	–	–	11000.5580	−6.7
	5/2		5/2	11654.3365	−3.0	11651.5552	−8.3	–	–
	3/2		3/2	11648.8657	2.4	11647.2333	1.7	10967.2272	−8.6
	1/2		1/2	11700.4745	−1.6	11687.9042	−1.4	11018.8522	7.3
$2_{12} \leftarrow 1_{11}$	7/2		5/2	11635.9662	2.7	11629.3861	−0.8	10958.6393	−4.0
	5/2		3/2	11599.2814	1.9	11600.4599	3.9	10921.9639	−2.4
	3/2		1/2	11645.3390	4.0	11636.7393	−8.1	10968.0337	2.2
	5/2		5/2	11617.4911	−1.7	11614.8178	3.1	–	–
	3/2		3/2	11612.5310	9.5	11610.8987	5.8	10935.2100	4.2
	1/2		1/2	11663.8951	−3.8	11651.3849	9.2	–	–
$3_{03} \leftarrow 2_{02}$	9/2		7/2	17467.8690	−4.0	17460.4278	−2.4	–	–
	7/2		5/2	17467.8690	5.7	17460.4278	5.0	–	–
	5/2		3/2	17458.7266	1.1	17453.2245	−0.8	–	–
	3/2		1/2	–	–	17453.2487	−3.4	–	–
	7/2		7/2	17431.1211	4.1	–	–	–	–
	5/2		5/2	17485.0552	−1.0	17473.9647	2.4	–	–
	3/2		3/2	17495.4363	2.6	17482.1623	−0.1	–	–
$3_{12} \leftarrow 2_{11}$	9/2		7/2	17499.0087	1.9	17491.0860	2.0	–	–
	7/2		5/2	17489.7860	1.1	17483.8214	3.1	–	–
	5/2		3/2	17489.5532	−4.0	17483.6406	2.6	–	–
	3/2		1/2	17498.7050	−3.0	17490.8531	−2.0	–	–
	7/2		7/2	17471.6077	−1.2	17469.4855	0.0	–	–
	5/2		5/2	17502.5949	5.8	17493.9116	7.5	–	–
	3/2		3/2	17516.9775	0.3	17505.2400	−3.9	–	–
$3_{13} \leftarrow 2_{12}$	9/2		7/2	17444.1532	−1.8	17436.2985	−2.0	–	–
	7/2		5/2	17434.9328	−0.3	17429.0359	1.1	–	–
	5/2		3/2	17434.6314	–1.3	17428.7956	0.3	–	–
	3/2		1/2	17443.7803	−3.1	17436.0108	−1.6	–	–
	7/2		7/2	17416.4577	−4.7	17414.4609	−1.7	–	–
	5/2		5/2	17447.8761	1.4	17439.2285	−3.7	–	–
	3/2		3/2	17462.3487	1.5	17450.6396	−1.0	–	–

[a] $\Delta\nu = \nu_{obs} - \nu_{calcd}$.

Values of the spectroscopic constants determined for each of the isotopomers $H_2O\cdots{}^{35}ClF$, $H_2O\cdots{}^{37}ClF$, $H_2{}^{18}O\cdots{}^{35}ClF$, $D_2O\cdots{}^{35}ClF$, $D_2O\cdots{}^{37}ClF$, $HDO\cdots{}^{35}ClF$ and $HDO\cdots{}^{37}ClF$ from the final cycles of the least-squares fits conducted using the program devised by Pickett[15] are included in Table 3. For all but the HDO-based isotopomers, the diagonal components $\chi_{aa}(Cl)$ and $\{\chi_{bb}(Cl) - \chi_{cc}(Cl)\}$ of the Cl nuclear quadrupole coupling tensor $\chi_{\alpha\beta} = -\{eQ(Cl)/h\}V_{\alpha\beta}$, where $V_{\alpha\beta} = -\partial^2 V/\partial\alpha\partial\beta$ and α, $\beta = a$, b or c, were both determinable. In view of the small value of $\{\chi_{bb}(Cl) - \chi_{cc}(Cl)\}$ and the expected nearly negligible contribution of spin-rotation coupling to observed hyperfine frequencies, the components $M_{bb}(Cl)$ and $M_{cc}(Cl)$ of the spin-rotation coupling tensor $\mathbf{M}(Cl)$ were constrained to be equal. We note that $M_{aa}(Cl)$ is barely determinable. The availability of only a single set of $J+1 \leftarrow J$ transitions for $H_2{}^{18}O\cdots{}^{35}ClF$ required the reasonable assumption that Δ_J is unchanged from $H_2O\cdots{}^{35}ClF$ to allow B_0, C_0 and Δ_{JK} to be determined separately. For isotopomers involving HDO, the absence of $K_{-1} = 1$ transitions meant that only $(B_0 + C_0)/2$, Δ_J and $\chi_{aa}(Cl)$ were determinable. Also included in Table 3 is the standard deviation σ of the fit for each isotopomer. This quantity is of the same order of magnitude as the estimated accuracy of frequency measurement in each case and indicates a satisfactory choice of Hamiltonian.

Transitions of $H_2O\cdots F_2$ showed evidence of a complicated and only partially resolved hyperfine structure that could be accounted for by assigning its origin to the magnetic coupling of the spin vectors $\boldsymbol{I}_F$ of the two F atoms to the framework angular momentum $\boldsymbol{J}$ (i.e. to spin-spin and spin-rotation coupling of the F nuclei). This hyperfine structure for the parent isotopomer was just well enough resolved to encourage an attempt to analyse it. Frequencies of the hyperfine components for the $J = 2 \leftarrow 1$ and $J = 3 \leftarrow 2$ sets of R-branch transitions are given in Table 4. The Hamiltonian employed in their least-squares analysis to generate spectroscopic constants was given by Equation (2), where $\mathbf{D}(F_i,F_o)$ is the F_i,F_o

$$H = H_R - \boldsymbol{I}_{Fi}\mathbf{D}(F_i,F_o)\boldsymbol{I}_{Fo} + \boldsymbol{I}_{Fi}\mathbf{M}(F_i)\boldsymbol{J} + \boldsymbol{I}_{Fo}\mathbf{M}(F_o)\boldsymbol{J} \quad (2)$$

Table 2. Observed and calculated rotational transition frequencies of HDO···^{35}ClF, HDO···^{37}ClF, D_2O···^{35}ClF and D_2O···^{37}ClF.

$J'_{K_{-1}K_1} \leftarrow J''_{K_{-1}K_1}$	F'	←	F''	HDO···^{35}ClF		HDO···^{37}ClF		D_2O···^{35}ClF		D_2O···^{37}ClF	
				ν_{obs} [MHz]	$\Delta\nu$[a] [kHz]	ν_{obs} [MHz]	$\Delta\nu$[a] [kHz]	ν_{obs} [MHz]	$\Delta\nu$[a] [kHz]	ν_{obs} [MHz]	$\Delta\nu$[a] [kHz]
$2_{02} \leftarrow 1_{01}$	7/2		5/2	11155.4673	0.7	11148.4243	4.0	10731.5402	2.8	10722.9235	−5.0
	5/2		3/2	–	–	–	–	–	–	–	–
	3/2		1/2	11115.6477	−2.2	11117.0222	−6.5	10691.7323	2.1	10691.5464	3.0
	5/2		5/2	11118.7424	1.5	11119.4759	2.4	10694.8229	3.6	–	–
	3/2		3/2	11181.7692	−0.1	11169.1373	0.5	10757.8374	−3.6	10743.6596	9.0
	1/2		1/2	11152.2888	−1.2	11145.9191	−0.4	10728.3602	−2.1	10720.4324	−0.1
	1/2		3/2	11218.4106	1.2	–	–	–	–	–	–
$2_{11} \leftarrow 1_{10}$	7/2		5/2	–	–	–	–	10765.8989	−3.1	10756.0139	0.0
	5/2		3/2	–	–	–	–	10729.2542	2.7	10727.1144	0.6
	3/2		1/2	–	–	–	–	10775.5796	−1.2	10763.6301	−0.4
	5/2		5/2	–	–	–	–	10747.7271	0.1	10741.6826	−3.0
	3/2		3/2	–	–	–	–	10742.2904	2.2	10737.3905	4.3
	1/2		1/2	–	–	–	–	10793.8605	2.2	–	–
$2_{12} \leftarrow 1_{11}$	7/2		5/2	–	–	–	–	10709.1744	7.6	10699.4087	2.5
	5/2		3/2	–	–	–	–	10672.5118	−4.5	10670.5019	−4.2
	3/2		1/2	–	–	–	–	10718.5591	−3.2	10706.7887	−3.1
	5/2		5/2	–	–	–	–	10690.7254	−5.5	10684.8615	−3.6
	3/2		3/2	–	–	–	–	10685.7374	−2.1	–	–
	1/2		1/2	–	–	–	–	10737.1027	1.9	–	–
$3_{03} \leftarrow 2_{02}$	9/2		7/2	16729.9186	−2.9	16719.9875	0.7	16094.0332	−3.6	16081.7586	3.7
	7/2		5/2	–	–	–	–	–	–	–	–
	5/2		3/2	16720.7836	6.3	16712.7842	−2.9	16084.8968	3.5	16074.5494	−8.1
	3/2		1/2	–	–	–	–	16084.9469	3.6	–	–
	7/2		7/2	16693.1856	−0.3	16691.0374	4.2	16057.3108	1.6	16052.8150	5.3
	5/2		5/2	16747.0960	−2.2	16733.5157	0.2	16111.2102	−5.0	16095.2848	−5.6
	3/2		3/2	16757.4641	−0.8	16741.7047	−2.2	16121.5734	2.0	–	–
$3_{12} \leftarrow 2_{11}$	9/2		7/2	–	–	–	–	16139.1172	3.3	16126.2909	3.2
	7/2		5/2	–	–	–	–	16129.8916	−5.3	16119.0250	−4.2
	5/2		3/2	–	–	–	–	16129.6602	−6.3	–	–
	3/2		1/2	–	–	–	–	16138.8079	−1.1	–	–
	7/2		7/2	–	–	–	–	16111.7211	−0.8	–	–
	5/2		5/2	–	–	–	–	16142.7055	2.3	–	–
	3/2		3/2	–	–	–	–	16157.0927	6.1	–	–
$3_{13} \leftarrow 2_{12}$	9/2		7/2	–	–	–	–	16053.9913	1.3	16041.3617	2.7
	7/2		5/2	–	–	–	–	16044.7708	−2.2	16034.1035	3.0
	5/2		3/2	–	–	–	–	16044.4802	2.2	–	–
	3/2		1/2	–	–	–	–	16053.6219	1.4	–	–
	7/2		7/2	–	–	–	–	16026.3340	–3.0	–	–
	5/2		5/2	–	–	–	–	16057.7052	4.1	–	–
	3/2		3/2	–	–	–	–	–	–	–	–

[a] $\Delta\nu = \nu_{obs} - \nu_{calcd}$.

Table 3. Ground-state spectroscopic constants determined for seven isotopomers of the $H_2O\cdots ClF$ complex.

Spectroscopic constant	Isotopomer						
	$H_2O\cdots{}^{35}ClF$	$H_2O\cdots{}^{37}ClF$	$H_2{}^{18}O\cdots{}^{35}ClF$	$D_2O\cdots{}^{35}ClF$	$D_2O\cdots{}^{37}ClF$	HDO···^{35}ClF[a]	HDO···^{37}ClF[a]
A_0 [MHz][b]	308267	308227	307344	159373	159339	212038	211990
B_0 [MHz]	2920.2516(3)	2919.0626(3)	2749.2929(5)	2696.3186(3)	2694.3030(4)	2788.1128(5)	2786.5199(5)
C_0 [MHz]	2901.9630(3)	2900.7976(3)	2733.1662(4)	2667.9398(3)	2665.9901(4)	–	–
Δ_J [kHz]	4.915(14)	4.969(15)	(4.915)[c]	4.492(15)	4.581(20)	4.743(26)	4.767(28)
Δ_{JK} [kHz]	−251.88(14)	−255.05(15)	−259.3(3)	−51.59(14)	−54.72(22)	–	–
χ_{aa}(Cl) [MHz]	−146.985(3)	−115.857(3)	−146.981(5)	−146.884(3)	−115.774(4)	−146.907(3)	−115.782(4)
$[\chi_{bb}(Cl) - \chi_{cc}(Cl)]$ [MHz]	−1.178(5)	−0.957(6)	−1.119(9)	−1.044(6)	−0.851(8)	–	–
M_{aa}(Cl) [kHz]	−2.6(10)	−6.1(11)	−2.6	−0.3(10)	−2.2(12)	–	–
$M_{bb}(Cl) = M_{cc}(Cl)$ [kHz]	4.06(22)	3.91(23)	3.1(4)	3.52(22)	1.6(3)	4.0(3)	3.0(7)
N[d]	38	36	14	36	30	11	10
σ [kHz][e]	3.2	3.9	5.2	3.5	4.2	2.4	3.1

[a] Only $(B+C)/2$, χ_{aa}(Cl), M_{bb}(Cl) and Δ_J available for HDO species since only $K_{-1}=0$ transitions were observed. [b] Value fixed at that calculated from experimental geometry given in Table 8 (see text). [c] Assumed. [d] Number of transitions included in the fit. [e] Standard deviation of fit.

0947-6539/01/0711-2298 $ 17.50+.50/0 *Chem. Eur. J.* **2001**, *7*, No. 11

Table 4. Observed and calculated rotational transition frequencies of $H_2O\cdots F_2$.

$J'_{K_{-1}K_1} \leftarrow J''_{K_{-1}K_1}$	I'	F'	←	I''	F''	$H_2O\cdots F_2$	
						ν_{obs} [MHz]	$\Delta\nu$[a] [kHz]
$2_{02} \leftarrow 1_{01}$	1	3		1	2	11892.1319	8.3
	1	1		1	0	–	–
	1	2		1	2	–	–
	1	1		1	1	–	–
	1	1		1	2	11892.0497	−3.0
	0	2		0	1	11892.1040	−1.5
$2_{11} \leftarrow 1_{10}$	1	3		1	2	11907.0657	2.2
	1	2		1	1	11906.9730	1.0
	1	1		1	0	11906.9797	−0.5
	1	2		1	2	–	–
	1	1		1	1	11906.9830	−8.6
	0	2		0	1	11907.0237	−1.2
$2_{12} \leftarrow 1_{11}$	1	3		1	2	–	–
	1	2		1	1	11847.3747	5.4
	1	1		1	0	11847.3747	−2.8
	1	2		1	2	–	–
	1	1		1	1	–	–
	0	2		0	1	11847.4242	2.0
$3_{03} \leftarrow 2_{02}$	1	4		1	3	17836.9568	10.4
	1	2		1	1	17836.8970	−11.0
	1	3		1	3	–	–
	1	2		1	2	–	–
	0	3		0	2	17836.9279	−1.0
$3_{12} \leftarrow 2_{11}$	1	4		1	3	–	–
	1	3		1	2	17859.3010	6.3
	1	2		1	1	17859.2798	4.7
	1	3		1	3	17859.2798	−7.7
	1	2		1	2	–	–
	0	3		0	2	17859.3010	−6.9
$3_{13} \leftarrow 2_{12}$	1	4		1	3	–	–
	1	3		1	2	–	–
	1	2		1	1	17769.8696	−1.5
	1	3		1	3	–	–
	1	2		1	2	–	–
	0	3		0	2	17769.9076	3.7

[a] $\Delta\nu = \nu_{obs} - \nu_{calcd}$.

Table 5. Properties of the free molecules F_2, ClF and H_2O used in the characterisation of $H_2O\cdots F_2$ and $H_2O\cdots ClF$.

Molecule	B_0 [MHz]	C_0 [MHz]	χ_0(Cl)[MHz]	$D_0(F_2)$[kHz]	M_0(F)[kHz]	r_0 geometry
$H_2{}^{16}O$[a]	435357.7	276138.7	–	–	–	r(O–H)
$H_2{}^{18}O$[a]	435331.6	276950.5	–	–	–	= 0.9650 Å[b]
HDO[a]	272912.6	192055.3	–	–	–	∢HOH = 104.8?
D_2O[a]	218038.2	145258.0	–	–	–	
$D_2{}^{18}O$[c]	218045.2	144201.7				
^{35}ClF	15418.251[d]	15418.251	−145.8718[e]	–	–	1.63176 Å[f]
^{37}ClF	15125.652[d]	15125.652	−114.9613[e]	–	–	1.63173 Å[f]
F_2	26481(1)[g]	26481(1)	–	−81.7(10)[h]	157.3(8)[h]	1.41744(6) Å[g]

[a] Ref. [21]. [b] The r_0 geometry of H_2O is the mean of the three determined for the $H_2{}^{16}O$ isotopomer in ref. [21] by using the three possible combinations (I_a, I_b), (I_b, I_c) and (I_a, I_c) of the principal moments of inertia. The ranges are ± 0.007 Å and 1.7° in r(O–H) and ∢HOH, respectively. [c] Ref. [38]. [d] Ref. [22]. [e] Ref. [39]. [f] Calculated from B_0 by using $r_0 = \{h/8\pi^2\mu B_0\}^{1/2}$. [g] Ref. [16]. [h] Ref. [17].

spin–spin coupling tensor and $\mathbf{M}(F_i)$ and $\mathbf{M}(F_o)$ are the spin–rotation coupling tensors associated with the inner (i) and outer (o) fluorine nuclei, respectively. These tensors have more components than could be satisfactorily determined with the frequencies of the partially resolved hyperfine components available in Table 4. In view of the fact that $H_2O\cdots F_2$ is very weakly bound (see below), it is reasonable to assume that, to a sufficient approximation, $M_{\alpha\alpha}(F_i) = M_{\alpha\alpha}(F_o)$ for $\alpha = a$, b and c. The effect of the F_2 angular oscillation on the values of $M_{bb}(F_x)$ and $M_{cc}(F_x)$ (x = i or o) will be well described by the usual projection formula as given in Equation (3), where $B + C$ is the complex rotational constant,

$$M_{bb}(F_x) = \tfrac{1}{4}\{(B+C)/B_{F_2}\}M_0(F) < 1 + \cos^2\gamma > \quad (3)$$

B_{F_2} is that of the free F_2 molecule[16] and $M_0(F)$ is the spin–rotation coupling constant of the free F_2 molecule,[17] (both given in Table 5). γ is the instantaneous angle between the F–F internuclear axis and the a axis of the complex. Fortunately, values of $M_{bb}(F_x)$ and $M_{cc}(F_x)$ predicted by Equation (3) are not a sensitive function of $\gamma_{av} = \cos^{-1}\langle\cos^2\gamma\rangle^{1/2}$ for a reasonable choice of range for this quantity. For example, $\gamma_{av} = 20(5)^\circ$ leads to −16.6(5) kHz for $M_{bb}(F_x)$ and $M_{cc}(F_x)$. Since γ_{av} is almost certain to lie in this range for the weakly bound $H_2O\cdots F_2$, we shall assume $M_{bb}(F_x) = M_{cc}(F_x) =$ −16.6(5) kHz.

Of the components of the spin–spin coupling tensor $\mathbf{D}(F_i,F_o)$, only $D_{aa}(F_i,F_o)$ is likely to be determinable from the hyperfine structure in the observed transitions of the nearly prolate asymmetric rotor $H_2{}^{16}O\cdots F_2$. Accordingly, this hyperfine structure was fitted under the assumptions described to give B_0, C_0, Δ_J, Δ_{JK} and $D_{aa}(F_i, F_o)$, the values of which from the final cycle of the analysis are shown in Table 6. Pickett's program[15] was employed and the coupled basis $\boldsymbol{I}_{Fi} + \boldsymbol{I}_{Fo} = \boldsymbol{I}$, $\boldsymbol{I} + \boldsymbol{J} = \boldsymbol{F}$ was chosen. The value of $D_{aa}(F_i, F_o)$ is related to that $D_0(F_2)$ of the free F_2 molecule[17] (given in Table 5) by the familiar expression given in Equation (4).

$$D_{aa}(F_i, F_o) = \tfrac{1}{2}D_0(F_2)\langle 3\cos^2\gamma - 1\rangle \quad (4)$$

Table 6. Ground-state spectroscopic constants determined for five isotopomers of the $H_2O\cdots F_2$ complex.

Spectroscopic constant	Isotopomer				
	$H_2{}^{16}O\cdots F_2$	$H_2{}^{18}O\cdots F_2$	$D_2O\cdots F_2$	$D_2{}^{18}O\cdots F_2$	$HDO\cdots F_2$[a]
A_0 [MHz][b]	332119	331155	170448	169639	228013
B_0 [MHz]	2988.0910(4)	2816.183(2)	2751.650(2)	2616.905(2)	2844.479[c]
C_0 [MHz]	2958.2896(4)	2789.767(2)	2707.633(2)	2577.213(2)	–
Δ_J [kHz]	20.49(2)	18.17(11)	16.8(3)	14.81(8)	18.7
Δ_{JK} [MHz]	−3.7205(2)	3.269(1)	3.771(3)	3.4221(8)	–
$M_{aa}(F_x)$ [kHz][d]	−91.6(6)	–	–	–	–
$M_{bb}(F_x)$ [kHz][d]	16.6	–	–	–	–
$D_{aa}(F_i,F_o)$ [kHz]	−68(4)	–	–	–	–
N[e]	22	6	6	6	2
σ [kHz][f]	5.1	6.1	6.8	4.7	–

[a] Only two $K_{-1}=0$ transitions were measured for this isotopomer. Hence only $(B+C)/2$ and Δ_J could be determined. No estimate of errors is available. [b] Fixed at value calculated from the experimental geometry given in Table 8. [c] $(B_0+C_0)/2$. [d] Values of $M_{bb}(F_i)=M_{bb}(F_o)=M_{cc}(F_i)=M_{cc}(F_o)=16.6$ kHz fixed in the fit. See text for justification. [e] Number of transitions in fit. [f] Standard deviation of the fit.

If $\gamma_{av}=20(5)^\circ$, as assumed earlier, Equation (4) predicts $D_{aa}(F_i, F_o)=-67(6)$ kHz, in excellent agreement with that, −68(4) kHz, observed.

For the remaining isotopomers of $H_2O\cdots F_2$, the hyperfine structure was insufficiently resolved and no attempt at analysis was made. Instead, the unperturbed centre frequency of each transition, as given in Table 7, was estimated from the centre of gravity of the partially resolved structure. The error of frequency measurement was then estimated to be 5 kHz. The spectroscopic constants B_0, C_0, Δ_J and Δ_{JK} determined by analysis of the $J=2\leftarrow1$ and $J=3\leftarrow2$ transitions for each of the isotopomers $H_2{}^{18}O\cdots F_2$, $D_2O\cdots F_2$ and $D_2{}^{18}O\cdots F_2$ are included in Table 6. For $HDO\cdots F_2$, no $K_{-1}=1$ transitions were observed and hence only $(B_0+C_0)/2$ and Δ_J could be obtained.

An interesting point to note when comparing the spectroscopic constants of $H_2O\cdots ClF$ and $H_2O\cdots F_2$ given in Tables 3 and 6, respectively, is that Δ_{JK} is negative for $H_2O\cdots ClF$, while it has the more usual positive sign for $H_2O\cdots F_2$. This fact has significant implications for the potential energy $V(\phi)$ as a function of the out-of-plane angle ϕ (see Figure 1) for $H_2O\cdots ClF$ and will be considered below.

Geometry of $H_2O\cdots ClF$ and $H_2O\cdots F_2$: The changes in the observed ground-state rotational constants B_0 and C_0 of $H_2O\cdots{}^{35}ClF$ that accompany isotopic substitution to give $H_2O\cdots{}^{37}ClF$, $D_2O\cdots{}^{35}ClF$ and $H_2{}^{18}O\cdots{}^{35}ClF$ establish that the order of the nuclei is as written, with O adjacent to Cl. Likewise, isotopic substitution in $H_2O\cdots F_2$ indicates that the weak interaction is between O and F. The fact that for $HDO\cdots{}^{35}ClF$ the rotational constant $\frac{1}{2}(B_0+C_0)=2788.1128$ MHz is close to the mean of the corresponding quantities 2911.0895 MHz and 2682.1292 MHz for $H_2O\cdots{}^{35}ClF$ and $D_2O\cdots{}^{35}ClF$ provides strong evidence that the two H atoms in $H_2O\cdots ClF$ are equivalent. The same relationship also holds for the values of $\frac{1}{2}(B_0+C_0)$ among $H_2O\cdots F_2$, $D_2O\cdots F_2$ and $HDO\cdots F_2$ (Table 6).

The observations alluded to in the preceding paragraph are consistent with geometries for $H_2O\cdots ClF$ and $H_2O\cdots F_2$ of the general type shown in Figure 1. It remains to establish the details, and in particular whether the out-of-plane angle ϕ is zero at equilibrium (i.e. whether the equilibrium geometry is C_{2v}, planar) or whether $\phi\neq0$ (i.e. whether the equilibrium geometry is of C_s symmetry, with a pyramidal configuration at O). In fact, nuclear spin statistical weight effects observed in the ground-state rotational spectra of both $H_2O\cdots ClF$ and $H_2O\cdots F_2$ show that, even if the equilibrium geometries are of C_s symmetry, the vibrational wavefunctions can be classified through the C_{2v} point group. This means that the potential energy barrier at the planar conformation ($\phi=0^\circ$) is low enough that tunnelling occurs at a significant frequency

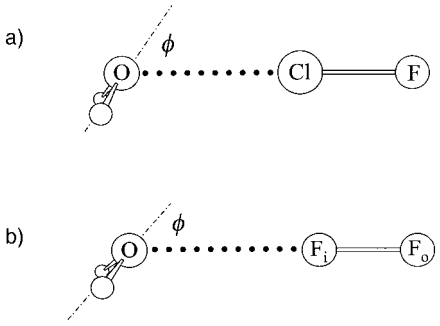

Figure 1. The geometries of a) $H_2O\cdots ClF$ and b) $H_2O\cdots F_2$ determined experimentally in the zero-point state. The drawings are to scale. In a), $\phi=58.9(16)^\circ$ and $r(O\cdots Cl)=2.6081(23)$ Å and in b) $\phi=48.5(21)^\circ$ and $r(O\cdots F_i)=2.7480(27)$ Å (i = inner). Both complexes have an equilibrium geometry of C_s symmetry with a pair of equivalent conformers having a pyramidal configuration at O and separated by a low potential energy barrier at the C_{2v} planar form.

Table 7. Observed and calculated rotational transition frequencies for four isotopomers of $H_2{}^{18}O\cdots F_2$.

$J'_{K_{-1}K_1}\leftarrow J''_{K_{-1}K_1}$	$H_2{}^{18}O\cdots F_2$		$D_2O\cdots F_2$		$D_2{}^{18}O\cdots F_2$		$HDO\cdots F_2$	
	ν_{obs} [MHz]	$\Delta\nu$[a] [kHz]	ν_{obs} [MHz]	$\Delta\nu$[a] [kHz]	ν_{obs} [MHz]	$\Delta\nu$[a] [kHz]	ν_{obs} [MHz]	$\Delta\nu$[a] [kHz]
$2_{12}\leftarrow1_{11}$	11171.8239	−3.5	10858.9340	−5.7	10334.3787	−3.9	–	–
$2_{02}\leftarrow1_{01}$	11211.3233	5.8	10918.0310	0.1	10387.7404	−0.1	11377.3150	0.0
$2_{11}\leftarrow1_{10}$	11224.6564	−2.3	10946.9799	5.7	10413.7713	4.0	–	–
$3_{13}\leftarrow2_{12}$	16756.6523	2.3	16287.4172	3.8	15500.6736	2.6	–	–
$3_{03}\leftarrow2_{02}$	16815.8790	−3.9	16376.0375	0.0	15580.6653	0.1	17064.8449	0.0
$3_{12}\leftarrow2_{11}$	16835.8986	1.6	16419.4613	−3.8	15619.7455	−2.6	–	–

[a] $\Delta\nu=\nu_{obs}-\nu_{calcd}$.

0947-6539/01/0711-2300 $ 17.50+.50/0 *Chem. Eur. J.* **2001**, *7*, No. 11

between the two equivalent C_s conformers and the $v=0$ and $v=1$ states are nondegenerate. The complex is then sometimes referred to as *effectively* planar.[7]

Whether $H_2O\cdots ClF$ and $H_2O\cdots F_2$ are planar or effectively planar complexes, the operation C_2^a exchanges a pair of equivalent protons. If $\boldsymbol{I}_1$ and $\boldsymbol{I}_2$ are the proton nuclear spin vectors, detailed arguments reveal that in the vibrational ground state only the singlet spin state $\boldsymbol{I}_1+\boldsymbol{I}_2=0$ can occur in combination with $K_{-1}=0$ rotational states. Conversely, only triplet spin states $|\boldsymbol{I}_1+\boldsymbol{I}_2|=1$ appear with $K_{-1}=1$ rotational states. Accordingly, a nuclear spin statistical weight ratio of 3:1 for $K_{-1}=1$ relative to $K_{-1}=0$ states is required if $H_2O\cdots ClF$ and $H_2O\cdots F_2$ are planar or effectively planar.

Since collisional transfer between triplet and singlet states of H_2O is forbidden during the supersonic expansion,[18] the $K_{-1}=1$ states of the complexes will tend to retain their room-temperature populations. Evidently, within a given $(J+1)\leftarrow J$ group of transitions, those involving $K_{-1}=1$ should, in the absence of significant rotational cooling, be more intense than the $K_{-1}=0$ transition by a factor of approximately 3. In fact, $K_{-1}=1$ transitions are observed to be stronger than the $K_{-1}=0$ transition in isotopomers of $H_2O\cdots ClF$ and $H_2O\cdots F_2$ that contain the H_2O subunit, but a quantitative measurement of the effect is difficult because the rotational temperature is unknown. Moreover, for species based on D_2O, the order of the relative intensities is reversed, a result consistent with the 1:2 nuclear spin statistical weight ratio required by exchange of a pair of $I=1$ bosons. We note that collisional transfer between $K_{-1}=2$ and $K_{-1}=0$ states (both of which occur in combination with singlet nuclear spin functions) is allowed and therefore rotational cooling of $K_{-1}=2$ states is efficient. Hence, $K_{-1}=2$ transitions are not observed. Likewise, in species containing HDO the two hydrogen nuclei are no longer equivalent and there is no collisional propensity rule forbidding $K_{-1}=1$ to $K_{-1}=0$ transfer. Therefore, $K_{-1}=1$ levels are efficiently cooled, in agreement with our failure to observe $K_{-1}=1$ transitions in HDO containing isotopomers. In the limit of a high potential energy barrier at $\phi=0$, the vibrational levels $v=0$ and $v=1$ become degenerate and nuclear spin statistical weight alternations disappear. Thus, the observation of such alternations rules out a high potential energy barrier.

Ab initio calculations indicate that the changes in the geometries of the monomers H_2O, ClF and F_2 on formation of $H_2O\cdots ClF$ and $H_2O\cdots F_2$ are small, especially in the case of $H_2O\cdots F_2$. It has been shown elsewhere[19] that, for complexes such as these, it is better to obtain the parameters ϕ and $r(O\cdots Cl)$ or $r(O\cdots F_i)$ (Figure 1) that define the geometry by fitting I_b+I_c rather than the independent values I_b and I_c because of the more serious effects of zero-point vibrations in the latter case. Indeed, it was shown that the form of the contribution of the two water H atoms to I_b+I_c requires that this quantity leads to an effective value $\phi_{eff}=\cos^{-1}\langle\cos^2\phi\rangle^{1/2}$. Therefore, a least-squares fit to I_b+I_c of the seven isotopomers $H_2O\cdots{}^{35}ClF$, $H_2O\cdots{}^{37}ClF$, $H_2{}^{18}O\cdots{}^{35}ClF$, $D_2O\cdots{}^{35}ClF$, $D_2O\cdots{}^{37}ClF$, $HDO\cdots{}^{35}ClF$ and $HDO\cdots{}^{37}ClF$ was carried out with the program STRFIT[20] to give the results $r(O\cdots Cl)=2.6081(23)$ Å and $\phi_{eff}=58.9(16)^\circ$. The r_0 geometries of H_2O[21] and ClF[22] given in Table 5 were assumed unchanged, and the $O\cdots Cl$–F nuclei were assumed collinear, as indicated by the ab initio calculations. When the fit was repeated but with r_0(ClF) assumed to have increased by the amount 0.0166 Å found in the ab initio calculations (see next Section), the results were $r(O\cdots Cl)=2.5943(20)$ Å and $\phi_{eff}=58.4(14)^\circ$. Evidently, ϕ_{eff} is largely insensitive to assumptions about r(ClF), while $r(O\cdots Cl)$ is shortened pro rata. The changes in the H_2O geometry indicated by the ab initio calculations have a negligible effect by comparison, as do the changes in the H_2O r_0 geometry on deuteration. Interestingly, fitting I_b and I_c separately for the first five isotopomers (separate values are not available for $HDO\cdots{}^{35}ClF$ and $HDO\cdots{}^{37}ClF$) gives $r(O\cdots Cl)=2.6067(29)$ Å and $\phi_{eff}=58.2(20)^\circ$ when unperturbed monomer geometries are used.

The results obtained for $H_2O\cdots F_2$ by fitting I_b+I_c for the five isotopomers $H_2O\cdots F_2$, $H_2{}^{18}O\cdots F_2$, $D_2O\cdots F_2$, $D_2{}^{18}O\cdots F_2$ and $HDO\cdots F_2$ under the assumption of unchanged monomer geometries[16, 21] (see Table 5) are $r(O\cdots F_i)=2.7480(27)$ Å and $\phi_{eff}=48.5(21)^\circ$. If the lengthening of the F_2 internuclear distance of 0.0065 Å predicted by ab initio calculations (see next Section) is assumed, the results are $r(O\cdots F_i)=2.7426(27)$ Å and $\phi_{eff}=48.4(20)^\circ$. Fitting I_b and I_c for $H_2O\cdots F_2$, $H_2{}^{18}O\cdots F_2$, $D_2O\cdots F_2$ and $D_2{}^{18}O\cdots F_2$ by assuming unchanged monomers gives results that are somewhat less precise but identical within the experimental error, namely $r(O\cdots F_i)=2.742(9)$ Å and $\phi_{eff}=43.8(71)^\circ$.

The results from this section show that when ϕ_{eff} is determined from ground-state moments of inertia, both $H_2O\cdots ClF$ and $H_2O\cdots F_2$ are found to have a pyramidal configuration at O on average but it must be borne in mind that ϕ_{eff} is related to the zero-point average of $\cos^2\phi$ and would be non-zero even if these complexes were planar C_{2v} at equilibrium ($\phi_e=0$ but $\phi_{eff}>0$). It remains to determine whether the equilibrium geometries of $H_2O\cdots ClF$ and $H_2O\cdots F_2$ are planar C_{2v} ($\phi_e=0$) or pyramidal C_s ($\phi_e>0$) (see next Section).

Ab initio calculations for $H_2O\cdots ClF$ and $H_2O\cdots F_2$: To determine whether $H_2O\cdots ClF$ and $H_2O\cdots F_2$ have equilibrium geometries that are planar C_{2v} ($\phi_e=0$) or pyramidal C_s ($\phi_e>0$), we carried out ab initio calculations. The GAMESS package[23] was used for these calculations and the aug-cc-pVDZ basis set[24, 25] was chosen because it was developed specifically to deal with weakly bound complexes. Electron correlation was taken into account by using second-order Møller–Plesset perturbation theory.[26] Energies were corrected for basis set superposition error (BSSE) by the Boys–Bernardi counterpoise correction method.[27] The results of complete geometry optimisations are given in Table 8 for the monomers H_2O, ClF and F_2 and both complexes $H_2O\cdots ClF$ and $H_2O\cdots F_2$. Also included in Table 8 are the experimental equilibrium geometries of F_2,[16] ClF[28] and H_2O[29] and the effective values $r(O\cdots Cl)$, $r(O\cdots F_i)$ and ϕ_{eff} of the complexes determined by fitting ground-state values of I_b+I_c. The agreement between theory and experiment is good, but we are comparing equilibrium geometries from ab initio calculations with experimental zero-point effective parameters. The agreement with earlier ab initio calculations by Dahl and Røeg-

Table 8. Comparison of geometries of F_2, ClF, H_2O, $H_2O\cdots ClF$ and $H_2O\cdots F_2$ calculated at the aug-cc-pVDZ/MP2 level with those established experimentally.

Molecule	aug-cc-pVDZ/MP2 geometry	Experimental geometry
F_2	r_e(F–F) = 1.4253 Å	1.4131(8)[a]
ClF	r_e(Cl–F) = 1.6760 Å	1.628341(4)[b]
H_2O	r_e(O–H) = 0.9659 Å	0.957848(16)[c]
	$\angle_e$HOH = 103.67°	104.5424(46)
$H_2O\cdots ClF$	r_e(O–H) = 0.9673 Å	–
	$\angle_e$HOH = 104.33°	–
	r_e(Cl–F) = 1.6926 Å	–
	r_e(O–Cl) = 2.5291 Å	2.608(2) Å[d]
	r_e(O···F) = 4.2217 Å	4.240(2) Å
	ϕ = 55.8°[e]	58.9(16)°
	θ = 0.2°[f]	0.0 (assumed)
$H_2O\cdots F_2$	r_e(O–H) = 0.9660 Å	–
	$\angle_e$HOH = 103.80°	–
	r_e(F–F) = 1.4318 Å	–
	r_e(O···F_i) = 2.6002 Å	2.748(3) Å[d]
	r_e(O···F_o) = 4.0318 Å	4.166(3) Å
	ϕ = 40.5°[e]	48.5(20)°
	θ = 1.1°[f]	0.0 (assumed)

[a] Ref. [16]. [b] Ref. [28]. [c] Ref. [29]. [d] r_0 values calculated by assuming r_0 geometries of monomers unchanged (Table 5) and fitting observed moments of inertia $I_b + I_c$ (see text). [e] ϕ is the angle between the C_2 axis of H_2O and the O···F_i internuclear axis (i = inner, o = outer), as defined in Figure 1. [f] θ is the deviation of the O···Cl–F or O···F_i–F_o nuclei from collinearity, in the direction of the water H atoms (see Figure 1).

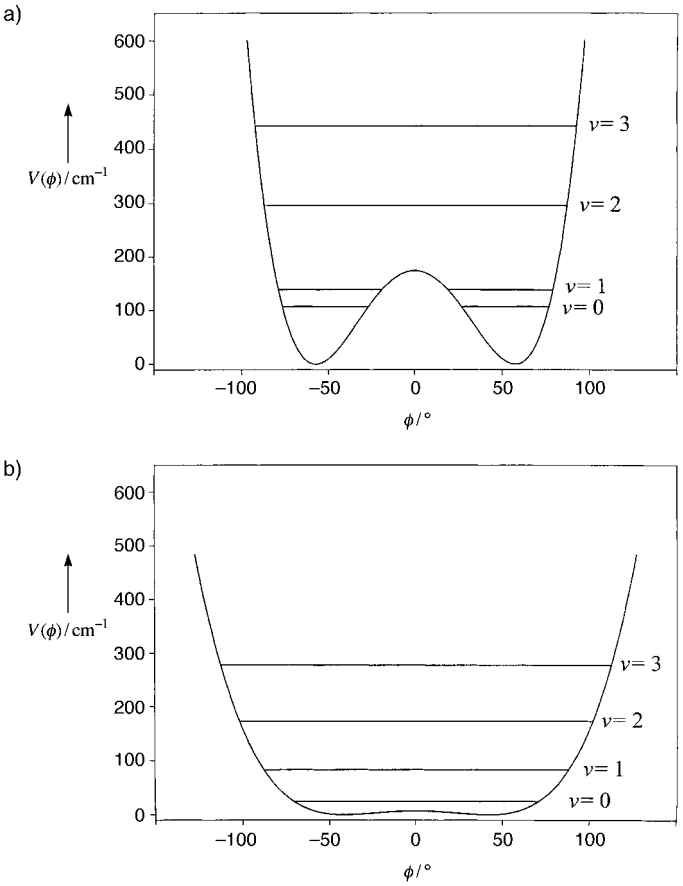

Figure 2. The potential energy $V(\phi)$ (expressed as a wavenumber) as a function of the angle ϕ (see Figure 1 for definition) for a) $H_2O\cdots ClF$ and b) $H_2O\cdots F_2$. The curves are of the form $V(\phi) = \alpha\phi^4 + \beta\phi^2$ and were obtained by least-squares fits to numerically generated points $\{V(\phi),\phi)\}$ obtained by ab initio calculations at the aug-cc-pVDZ/MP2 level of theory. See text for discussion.

gen[30] is satisfactory, although they find $H_2O\cdots F_2$ to have a planar geometry of C_{2v} symmetry.

A better comparison with experiment is possible if we consider the shape of the potential energy curve obtained when $V(\phi)$ is plotted as a function of the out-of-plane angle ϕ defined in Figure 1. The fact that the full optimisations leads to pyramidal geometries of C_s symmetry for both $H_2O\cdots ClF$ and $H_2O\cdots F_2$ implies that $V(\phi)$ is a double-minimum function. The crucial questions are then: How high is the potential energy barrier V_0 at the planar C_{2v} geometry, where is the zero-point energy level located with respect to the barrier, and can an appropriate ϕ_{eff} be estimated using this function?

The potential energy functions $V(\phi)$ for $H_2O\cdots ClF$ and $H_2O\cdots F_2$ shown in Figure 2 were generated ab initio as follows. Energies were determined as described above for the full optimisation, except that now the optimisation was carried out at each of a series of fixed values of ϕ in the range 0° to 80°. Corrections for BSSE were again applied. To determine the positions of the energy levels of a one-dimensional oscillator associated with each function, we fitted each numerical potential energy curve with the familiar quartic-quadratic potential given in Equation (5) which has been successful in describing the out-of-plane bending vibrations of cyclic molecules[31] and also intermolecular bending vibrations of the hydrogen-bonded complex $H_2O\cdots HF$.[32]

$$V(\phi) = \alpha\phi^4 + \beta\phi^2 \quad (5)$$

In fact, the $V(\phi)$ values obtained from the ab initio calculations could be quite accurately reproduced by Equation (5). Least-squares fits to the ab initio $V(\phi)$ values for $H_2O\cdots ClF$ yielded the results $\alpha = 173.2(15)\,cm^{-1}$ and $\beta = -347.6(26)\,cm^{-1}$, while for $H_2O\cdots F_2$ the corresponding values were $\alpha = 25.2(6)\,cm^{-1}$ and $\beta = -26.7(9)\,cm^{-1}$. It is then convenient to express $V(\phi)$ in terms of the reduced dimensionless coordinate z according to Equation (6) because the energy levels of a one-dimensional anharmonic oscillator governed by this function are readily calculated.[31, 33]

$$V(z) = a(z^4 + bz^2) \quad (6)$$

The relationships[32] between α, β, a and b are given by Equations (7) and (8), where μ is the reduced mass for the vibration, r_H is the O–H distance in H_2O and θ is the HOH angle.

$$a = \{(r_H\cos\tfrac{1}{2}\theta)^4(2\mu/\hbar^2)^2\}^{-1/3}\alpha^{1/3} \quad (7)$$

$$b = \{(r_H\cos\tfrac{1}{2}\theta)^2(2\mu/\hbar^2)\}^{-1}a^{-2}\beta \quad (8)$$

The expression for μ appropriate to a complex such as $H_2O\cdots HF$, $H_2O\cdots ClF$ or $H_2O\cdots F_2$ is given in ref. [32]. By using Equations (7) and (8) we obtain $a = 51.3\,cm^{-1}$ and $b = -3.69$ for $H_2O\cdots ClF$ and $a = 27.1\,cm^{-1}$ and $b = -1.02$ for

0947-6539/01/0711-2302 $ 17.50+.50/0 Chem. Eur. J. 2001, 7, No. 11

$H_2O\cdots F_2$. The energy levels $v=0,1,2$ and 3 obtained for the one-dimensional quartic-quadratic oscillator using these functions are drawn in Figure 2. The values of ϕ_e are 57.4° and 41.7° for these functions for $H_2O\cdots ClF$ and $H_2O\cdots F_2$, respectively.

Two conclusions are immediately evident from Figure 2. Firstly, for $H_2O\cdots ClF$ both energy levels $v=0$ and $v=1$ lie below the top of the potential energy barrier, which has a height $V_0=174\,cm^{-1}$ above the minima. In fact, the $v=1-0$ separation is $31\,cm^{-1}$. This is small enough that a significant Coriolis interaction between $K_{-1}=1$ levels of $v=0$ and $K_{-1}=0$ levels of $v=1$ is possible, given a sufficiently large Coriolis coupling constant and the fact that $K_{-1}=1$ levels of a given J lie at a wavenumber $c^{-1}(A-B)\approx 10\,cm^{-1}$ above the corresponding $K_{-1}=0$ level. This probably accounts for the sign of the observed value of the centrifugal distortion constant Δ_{JK} (see Table 4), negative values of which constant have also been observed in association with Coriolis interactions in $H_2O\cdots HF$.[34] We note that $c^{-1}(A-B)$ decreases to about $5\,cm^{-1}$ in $D_2O\cdots ClF$. Interestingly, Δ_{JK}, although still negative, is much reduced in magnitude in the D_2O species, indicating a reduced Coriolis interaction. Insufficient data precludes a more detailed analysis of this interesting effect, however.

The second conclusion from the functions $V(\phi)$ shown in Figure 2 is that for $H_2O\cdots F_2$ even the energy level $v=0$ lies $17\,cm^{-1}$ above the top of the potential energy barrier ($V_0=7\,cm^{-1}$). Thus, while $H_2O\cdots ClF$ can be reasonably described as pyramidal at O in the zero-point state, it is better to describe $H_2O\cdots F_2$ as planar. Nevertheless, both $H_2O\cdots ClF$ and $H_2O\cdots F_2$ have pyramidal equilibrium geometries and the equilibrium angles $\phi_e=57.4°$ and 41.7°, respectively, are consistent with the simple nonbonding electron-pair model for their angular geometries described in the Introduction.

Finally, it is of interest to obtain an estimate of ϕ in the zero-point state from the ab initio potential energy functions. While $\langle\phi\rangle_{v,v}$ is necessarily zero, the quantity $\langle\cos\phi\rangle_{v,v}$ is nonzero for a double-minimum potential energy function. Expansion of $\langle\cos\phi\rangle_{v,v}$ in a Taylor series leads to Equation (9).[19]

$$\langle\cos\phi\rangle_{v,v}=1-\tfrac{1}{2}\langle\phi^2\rangle_{v,v}+\tfrac{1}{24}\langle\phi^4\rangle_{v,v}-\cdots \qquad (9)$$

The relations $\phi=0.7377z$ and $\phi=1.018z$ for $H_2O\cdots ClF$ and $H_2O\cdots F_2$, respectively, are implied by the α and a values given earlier. Values of $\langle z^2\rangle_{0,0}$ and $\langle z^4\rangle_{0,0}$ have been tabulated as a function of the potential constant b and are available.[35] Hence $\langle\phi^2\rangle_{0,0}$ and $\langle\phi^4\rangle_{0,0}$ can be calculated and used in Equation (9) to give the operationally defined angles $\phi_0=\cos^{-1}\langle\cos\phi\rangle_{0,0}=45.4°$ and 37.9° for $H_2O\cdots ClF$ and $H_2O\cdots F_2$, respectively. Given that ϕ_{eff} obtained by fitting zero-point I_b+I_c values are approximately related to instantaneous values by $\phi_{eff}\approx\cos^{-1}\langle\cos^2\phi\rangle^{1/2}$, we expect reasonable, but not exact, agreement with ϕ_0 values. In fact, ϕ_0 is somewhat smaller than ϕ_{eff} in both cases. Indeed, here ϕ_e is closer to ϕ_{eff} than ϕ_0.

Strength of the intermolecular binding in $H_2O\cdots ClF$ and $H_2O\cdots F_2$: The equilibrium dissociation energies D_e obtained from the ab initio calculations discussed in the previous Section are 21.2 kJ mol^{-1} and 5.3 kJ mol^{-1} for $H_2O\cdots ClF$ and $H_2O\cdots F_2$, respectively. According to this criterion $H_2O\cdots ClF$ is four times more strongly bound than $H_2O\cdots F_2$. Such a result is not unexpected given that the dispersion interaction between H_2O and ClF is likely to be greater than that between H_2O and F_2. Moreover, ClF has an electric dipole moment while F_2 is nonpolar and has only a small electric quadrupole moment,[36] so the electrostatic component of the interaction will also be greater in $H_2O\cdots ClF$.

D_e measures the energy required to produce an infinite displacement from equilibrium along the dissociation coordinate, r. If k_σ is the intermolecular stretching force constant, $\frac{1}{2}k_\sigma\delta r^2$ is the energy required to produce a small displacement δr and hence $\frac{1}{2}k_\sigma$ is a measure of the energy required to produce a unit infinitesimal displacement along r. Millen has shown that for a planar asymmetric rotor complex $B\cdots XY$ of C_{2v} symmetry, k_σ is related to the centrifugal distortion constant Δ_J by Equation (10)[37], where B and C are rotational constants of the complex, $b=(B/B_B)+(B/B_{XY})$ and c has the corresponding definition in terms of the rotational constants C.

$$k_\sigma=(8\pi^2\mu/\Delta_J)\{B^3(1-b)+C^3(1-c)-\tfrac{1}{4}(B-C)^2(B+C)(2-b-c)\} \qquad (10)$$

This expression holds in the approximation of rigid subunits and neglect of cubic and higher potential constants. Equation (10) is chosen as appropriate from ref. [37] because the vibrational wavefunctions of the effectively planar complexes $H_2O\cdots ClF$ and $H_2O\cdots F_2$ can be classified according to the C_{2v} point group.

Values of k_σ for the various isotopomers of $H_2O\cdots ClF$ and $H_2O\cdots F_2$ estimated from the Δ_J values of Tables 3 and 6, respectively, are shown in Table 9. The ground-state rotational constants of the monomers H_2O,[21, 38] ClF[22] and F_2[16] were used and are collected in Table 5 for convenience. We note from Table 9 that the k_σ values for the five isotopomers

Table 9. A comparison of intermolecular stretching force constants k_σ[a] for several isotopomers of $H_2O\cdots ClF$ and $H_2O\cdots F_2$.

Isotopomer	$H_2O\cdots{}^{35}ClF$	$H_2O\cdots{}^{37}ClF$	$D_2O\cdots{}^{35}ClF$	$D_2O\cdots{}^{37}ClF$	$HDO\cdots{}^{35}ClF$	$HDO\cdots{}^{37}ClF$
k_σ [Nm^{-1}]	14.26(4)	14.16(4)	13.34(4)	13.12(6)	13.59(7)	13.57(8)
Isotopomer		$H_2O\cdots F_2$	$H_2{}^{18}O\cdots F_2$	$D_2O\cdots F_2$	$D_2{}^{18}O\cdots F_2$	$HDO\cdots F_2$
k_σ [Nm^{-1}]		3.66(1)	3.69(2)	3.74(2)	3.84(2)	3.60[b]

[a] The quoted errors are those propagated from Δ_J by using Equation (10), and do not reflect systematic errors in the model. [b] Only two transitions having $K_{-1}=0$ were fitted for this isotopomer and therefore no experimental error in Δ_J or k_σ can be given.

of $H_2O\cdots F_2$ are almost identical within experimental error. On the other hand, there is a systematic decrease in k_σ for $H_2O\cdots ClF$ with progressive substitution of H by D. This is undoubtedly the result of the sensitivity of Δ_J of $H_2O\cdots ClF$ to anharmonic coupling. We also note from Table 9 that k_σ for $H_2O\cdots {}^{35}ClF$ is close to four times that of $H_2O\cdots F_2$ and that the behaviour of k_σ as a criterion of binding strength parallels that of D_e.

Dynamics of the ClF subunits in $H_2O\cdots ClF$: The Cl-nuclear quadrupole coupling constant $\chi_{aa}(Cl)$ of $H_2O\cdots {}^{35}ClF$ may be used to give information about the ClF subunit dynamics. On forming the complex, the coupling constant $\chi_0(Cl)$ of free ClF[39] becomes modified because the electric field gradient (efg) at Cl changes as a result of the response of the ClF charge distribution to the electric field and its gradients due to the H_2O subunit. The ab initio calculations discussed above allow the change in efg at Cl of ClF to be estimated. The fractional change f in the efg at Cl along the ClF axis z on complex formation is estimated to be $f=0.0121$. If we assume that the zero-point coupling constant $\chi_0(Cl)$ changes by the same fraction, the modified coupling constant along the ClF axis, z, in the complex is $\chi_0'(Cl)=(1+f)\chi_0(Cl)=-147.64$ MHz. In a reasonable approximation, the observed value $\chi_{aa}(Cl)$ of the Cl-nuclear quadrupole coupling constant in the zero-point state of the complex is then given by Equation (11), where γ is the instantaneous angle between the a and z axes.

$$\chi_{aa}(Cl)=\tfrac{1}{2}\chi_0'(Cl)\langle 3\cos^2\gamma-1\rangle \qquad (11)$$

By using Equation (11), we estimate that $\gamma_{av}=\cos^{-1}\langle\cos^2\gamma\rangle^{1/2}=3.1^\circ$. This indicates that the angular motion of ClF in $H_2O\cdots ClF$ is small compared with that of H_2O. The value of $[V_{bb}(Cl)-V_{cc}(Cl)]/V_{aa}(Cl)$ is calculated to be 0.0067, which is in good agreement with the observed ratio $[\chi_{bb}(Cl)-\chi_{cc}(Cl)]/\chi_{aa}(Cl)=0.0080$. The corresponding results for the optimised planar C_{2v} geometry are $\gamma_{av}=4.3^\circ$ and $[V_{bb}(Cl)-V_{cc}(Cl)]/V_{aa}(Cl)=0.0100$.

Discussion

The complexes $H_2O\cdots ClF$ and $H_2O\cdots F_2$ have been isolated and characterised by using a fast-mixing nozzle in combination with a pulsed-jet, Fourier-transform microwave spectrometer. Both complexes have geometry of C_s symmetry at equilibrium, with a pyramidal arrangement at the oxygen atom. Ab initio calculations at the aug-cc-pVDZ/MP2 level of theory give reasonable agreement with the experimentally determined distances $r(O\cdots F_i)$ and $r(O\cdots Cl)$ in $H_2O\cdots F_2$ and $H_2O\cdots ClF$, respectively, given that the experimental values are of the ground-state effective type.

For $H_2O\cdots ClF$, the variation of the potential energy $V(\phi)$ with the angle ϕ obtained from the ab initio calculations shows that the barrier to the planar C_{2v} geometry ($\phi=0$) separating the two equivalent C_s conformers is 174 cm^{-1}. The zero-point vibrational energy level $v=0$ lies well below the top of the barrier and there is reasonable agreement between the effective value ϕ_0 of the angle and that estimated from the potential energy function. For $H_2O\cdots F_2$, the ab initio potential energy function $V(\phi)$ has only a very small potential energy hump (7 cm^{-1}) at $\phi=0$ and the zero-point energy level lies above the top of the barrier. Hence, while both complexes $H_2O\cdots ClF$ and $H_2O\cdots F_2$ are effectively planar in the zero-point state (in the sense described above), both have an equilibrium geometry that can be understood if the electrophilic end of $^{\delta+}Cl-F^{\delta-}$ or $^{\delta+}F\underset{\delta-}{\overset{\delta-}{}}F^{\delta+}$ seeks out the axis of one of the nonbonding electron pairs on O. An angle $\phi_e\approx 54^\circ$ would be expected on that basis. The results from the ab initio calculations are 55.8° and 40.5°, respectively. The smaller value of ϕ_e for $H_2O\cdots F_2$ is readily understood on the basis of the weakness of the H_2O/F_2 interaction. For a very weak complex, the barrier at the planar geometry becomes small and the two minima in the function $V(\phi)$ tend to merge with each other, so that ϕ_e decreases in magnitude. The effect was demonstrated earlier[13] from electrostatic modelling of the potential energy $V(\phi)$ as a function of intermolecular distance in $H_2S\cdots HF$.

The conclusion from the work reported here is that the properties determined for $H_2O\cdots ClF$ and $H_2O\cdots F_2$ are consistent with the recent proposal[9] that there exists a halogen bond $B\cdots XY$ that is analogous to the more familiar hydrogen bond $B\cdots HX$. This can be clearly illustrated by considering the potential energy function $V(\phi)$ of $H_2O\cdots HCl$, as determined by the methods described here,[19] and shown in Figure 3. Its shape, the positions of the minima and the height

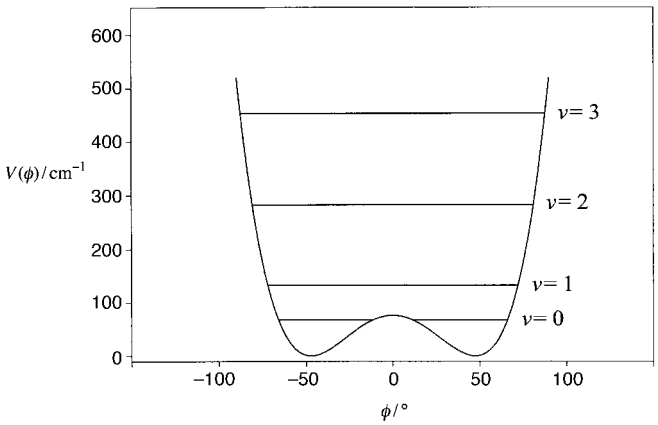

Figure 3. The potential energy $V(\phi)$ as a function of the angle ϕ for $H_2O\cdots HCl$. This curve[19] was obtained by the method summarised in the caption to Figure 2 and in the text.

of the barrier at the planar geometry are all similar to those of the function $V(\phi)$ for $H_2O\cdots ClF$ shown in Figure 2. All three complexes $H_2O\cdots HCl$, $H_2O\cdots F_2$, $H_2O\cdots ClF$ obey the rules set out in references [9, 13] but only when equilibrium geometries are used.

Experimental Section

The rotational spectra of $H_2O\cdots ClF$ and $H_2O\cdots F_2$ were observed and measured by using a pulsed-jet, Fourier-transform microwave spectrometer of the Balle-Flygare type[1, 2] but modified to include a fast-mixing nozzle[3] to generate the complexes. A mixture composed of approximately 1–2%

0947-6539/01/0711-2304 $ 17.50+.50/0 *Chem. Eur. J.* **2001**, *7*, No. 11

of either ClF (prepared by the method of Schack and Wilson)[40] or F_2 (99.8% pure; Distillers M.G.) in argon and held at a stagnation pressure of 3 bar was pulsed, via a Series 9 solenoid valve (Parker–Hannifin Corp.), down the outer of the two concentric, nearly coterminal tubes that constitute the mixing nozzle. Where this gas pulse emerged from the nozzle into the evacuated Fabry–Pérot cavity of the spectrometer, it encountered water vapour that issued continuously from the inner glass tube of the mixing nozzle. The water-vapour flow rate was the maximum possible from above a sample of the liquid at room temperature. Complexes of either $H_2O\cdots ClF$ or $H_2O\cdots F_2$ generated at the interface between the two gas flows as they emerged into the vacuum chamber were rotationally polarized by 1.1 μs pulses of microwave radiation and the subsequent free-induction decay at rotational transition frequencies was collected and processed in the usual way. For $H_2O\cdots ClF$ individual nuclear quadrupole hyperfine components had a half-width at half height of approximately 15–20 kHz and were measured with an estimated accuracy of 2 kHz. The partially resolved hyperfine structure arising from spin-spin and spin-rotation coupling of the various $I = 1/2$ nuclei in $H_2O\cdots F_2$ restricted the accuracy of frequency measurement to 5 kHz.

Isotopomers involving D_2O were generated by flowing the vapour from above a sample of deuterium oxide (Apollo Scientific Ltd) into the mixing nozzle. For HDO isotopomers, an equimolar mixture of D_2O and H_2O was employed. Samples of $H_2{}^{18}O$ and $D_2{}^{18}O$ allowed measurements on the isotopomers $H_2{}^{18}O\cdots ClF$, $H_2{}^{18}O\cdots F_2$ and $D_2{}^{18}O\cdots F_2$ to be made.

Acknowledgements

We thank the Engineering and Physical Sciences Research Council for studentships (S.A.C., C. M.E. and J.M.A.T.) and for a Senior Fellowship (A.C.L.). J.M.A.T. also thanks the Society of Chemical Industry for the award of a Messel Scholarship. The award of a grant from the E. U. Human Capital and Mobility Network SCAMP (Contract CHRX-CT 93–0157) to allow G.C. to work in the United Kingdom is gratefully acknowledged.

[1] T. J. Balle, W. H. Flygare, *Rev. Sci. Instrum.* **1981**, *52*, 33–45.
[2] A. C. Legon in *Atomic and Molecular Beam Methods*, *Vol. 2* (Ed.: G. Scoles), Oxford University Press, Oxford, **1992**, Chapter 9, pp. 289–308.
[3] A. C. Legon, C. A. Rego, *J. Chem. Soc. Faraday Trans.* **1990**, *86*, 1915–1921.
[4] G. H. Cady, *J. Am. Chem. Soc.* **1935**, *57*, 246–249.
[5] E. H. Appelman, *Acc. Chem. Res.* **1973**, *6*, 113–117.
[6] K. O. Christe, *Inorg. Chem.* **1972**, *11*, 1220–1222.
[7] S. A. Cooke, G. Cotti, J. H. Holloway, A. C. Legon, *Angew. Chem.* **1997**, *109*, 81–83; *Angew. Chem. Int. Ed. Engl.* **1997**, *36*, 129–130.
[8] S. A. Cooke, G. Cotti, C. M. Evans, J. H. Holloway, A. C. Legon, *Chem. Commun.* **1996**, 2327–2328.
[9] A. C. Legon, *Angew. Chem.* **1999**, *111*, 2850–2880; *Angew. Chem. Int. Ed.* **1999**, *38*, 2686–2714.
[10] A. C. Legon, *Chem. Phys. Lett.* **1999**, *314*, 472–480.
[11] A. C. Legon, *Chem. Eur. J.* **1998**, *4*, 1890–1897.
[12] A. C. Legon, D. J. Millen, *Faraday Discuss. Chem. Soc.* **1982**, *73*, 71–87.
[13] A. C. Legon, D. J. Millen, *Chem. Soc. Rev.* **1987**, *16*, 467–498.
[14] J. K. G. Watson, *J. Chem. Phys.* **1968**, *48*, 4517–4524.
[15] H. M. Pickett, *J. Mol. Spectrosc.* **1991**, *148*, 371–377.
[16] H. G. M. Edwards, E. A. M. Good, D. A. Long, *J. Chem. Soc. Faraday Trans. 2* **1976**, *72*, 984–987.
[17] I. Ozier, N. F. Ramsay, *Bull. Am. Phys. Soc.* **1966**, *11*, 23.
[18] A. C. Legon, *Faraday Discuss. Chem. Soc.* **1988**, *86*, 269–270.
[19] Z. Kisiel, B. A. Pietrewicz, P. W. Fowler, A. C. Legon, E. Steiner, *J. Phys. Chem. A.* **2000**, *104*, 6970–6978.
[20] Z. Kisiel,PROSPE – *Programs for Rotational Spectroscopy* database, http://info.ifpan.edu.pl/~kisiel/prospe.htm.
[21] R. L. Cook, F. C. DeLucia, P. Helminger, *J. Mol. Spectrosc.* **1974**, *53*, 62–76.
[22] J. C. McGurk, C. L. Norris, H. L. Tigelaar, W. H. Flygare, *J. Chem. Phys.* **1973**, *58*, 3118–3120.
[23] M. W. Schmidt, K. K. Baldridge, J. A. Boatz, S. T. Elbert, M. S. Gordon, J. H. Jensen, S. Koseki, N. Matsunaga, K. Nguyen, S. J. Su, T. L. Windus, M. Dupuis, J. A. Montgomery, *J. Comput. Chem.* **1993**, *14*, 1347–1363.
[24] T. H. Dunning, Jr., *J. Chem. Phys.* **1989**, *90*, 1007–1023.
[25] R. A. Kendall, T. H. Dunning, Jr., R. J. Harrison, *J. Chem. Phys.* **1992**, *96*, 6796–6806.
[26] C. Møller, M. S. Plesset, *Phys. Rev.* **1934**, *46*, 618–622.
[27] S. F. Boys, F. Bernardi, *Mol. Phys.* **1970**, *19*, 553–566.
[28] R. E. Willis, W. W. Clark, *J. Chem. Phys.* **1980**, *72*, 4946–4950.
[29] P. Jensen, S. A. Tashkun, V. G. Tyuterev, *J. Mol. Spectrosc.* **1994**, *168*, 271–289.
[30] T. Dahl, I. Røeggen, *J. Am. Chem. Soc.* **1996**, *118*, 4152–4158.
[31] J. Laane, *Appl. Spectrosc.* **1970**, *24*, 73–80.
[32] Z. Kisiel, A. C. Legon, D. J. Millen, *Proc. R. Soc. London A.* **1982**, *381*, 419–442.
[33] J. Mjöberg, Program ANHARM, University College London, **1975**.
[34] G. Cazzoli, P. G. Favero, D. G. Lister, A. C. Legon, D. J. Millen, Z. Kisiel, *Chem. Phys. Lett.* **1985**, *117*, 543–549.
[35] Z. Kisiel, Ph. D. Thesis, University of London, **1980**.
[36] S. A. Peebles, P. W. Fowler, A. C. Legon, unpublished results.
[37] D. J. Millen, *Can. J. Chem.* **1985**, *63*, 1477–1479.
[38] J. Bellet, W. J. Lafferty, G. Steenbeckeliers, *J. Mol. Spectrosc.* **1973**, *47*, 388–402.
[39] B. Fabricant, J. S. Muenter, *J. Chem. Phys.* **1977**, *66*, 5274–5277.
[40] C. J. Schack, R. D. Wilson, *Inorg. Synth.* **1986**, *24*, 1–3.

Received: November 13, 2000 [F2868]